An Ultrasonic Relaxation Study of 1-Alkyl-3-Methylmidazolium-Based Room Temperature Ionic Liquids: Probing the Role of Alkyl Chain Length in the Cation

Zorębski, M., Zorebski, E., Dzida, M., Skowronek, J., Jezak, S., Goodrich, P., & Jacquemin, J. (2016). An Ultrasonic Relaxation Study of 1-Alkyl-3-Methylmidazolium-Based Room Temperature Ionic Liquids: Probing the Role of Alkyl Chain Length in the Cation. The Journal of Physical Chemistry B. DOI: 10.1021/acs.jpcb.5b12635

Published in:
The Journal of Physical Chemistry B

Document Version:
Peer reviewed version

Queen's University Belfast - Research Portal:
Link to publication record in Queen's University Belfast Research Portal

THE JOURNAL OF PHYSICAL CHEMISTRY B

Article

An Ultrasonic Relaxation Study of 1-Alkyl-3-Methylmidazolium-Based Room Temperature Ionic Liquids: Probing the Role of Alkyl Chain Length in the Cation

Micha# Zor#bski, Edward Zorebski, Marzena Dzida, Justyna Skowronek, Sylwia Jezak, Peter Goodrich, and Johan Jacquemin

J. Phys. Chem. B, **Just Accepted Manuscript** • DOI: 10.1021/acs.jpcb.5b12635 • Publication Date (Web): 16 Mar 2016

An Ultrasonic Relaxation Study of 1-Alkyl-3-Methylimidazolium-Based Room Temperature Ionic Liquids: Probing the Role of Alkyl Chain Length in the Cation

Michał Zorębski[1], Edward Zorębski[1*], Marzena Dzida[1], Justyna Skowronek[1†], Sylwia Jężak[1†], Peter Goodrich[2], Johan Jacquemin[2]

[1] Institute of Chemistry, University of Silesia, Szkolna 9, 40-006 Katowice, Poland

[2] QUILL Research Centre, Queen's University of Belfast, Belfast BT95AG, Northern Ireland, UK

[*]Corresponding author. Tel.: +48 323591625; Fax: +48 322599978

E-mail address: emz@ich.us.edu.pl

Author Contributions

†These authors contributed equally to this work.

Abstract

Ultrasound absorption spectra of four 1-alkyl-3-methylimidazolium bis(trifluoromethylsulfonyl)imide were determined as a function of the alkyl chain length on the cation from 1-propyl- to 1-hexyl- from 293.15 to 323.15 K at ambient pressure. Herein, the ultrasound absorption measurements were carried out using a standard pulse technique within a frequency range from 10 to 300 MHz. Additionally the speed of sound, density and viscosity have been measured. The presence of strong dissipative processes during the ultrasound wave propagation was found experimentally, i.e. relaxation processes in the megahertz range were observed for all compounds over the whole temperature range. The relaxation spectra (both relaxation amplitude and relaxation frequency) were shown to be dependent on the alkyl side chain length of the 1-alkyl-3-methylimidazolium ring. In most cases, a single Debye model described the absorption spectra very well. However, a comparison of the determined spectra with the spectra of a few other imidazolium-based ionic liquids reported in the literature (in part recalculated in this work) shows that the complexity of the spectra increases rapidly with the elongation of the alkyl chain length on the cation. This complexity indicates that both the volume viscosity and the shear viscosity are involved in relaxation processes even in relatively low frequency ranges. As a consequence, the sound velocity dispersion is present at relatively low megahertz frequencies.

1. INTRODUCTION

Although relaxation processes in ionic liquids (ILs) have been extensively investigated over the last two decades using different experimental techniques, very few studies have been reported using an acoustic technique.[1-4] However, the acoustic technique is also an interesting method because the ultrasound absorption is related to the energy dissipation caused by various irreversible processes taking place in the liquids. This energy dissipation results in the characteristic spectra and a further analysis of such spectra, especially in a wide frequency range, can be an integral and significant source of valuable information regarding the molecular structure of the liquids, as well as, the various physical and chemical processes occurring in the liquids at a nearly ideal thermal equilibrium.[5] Ultrasound absorption investigations are also very useful and informative in the case of the pressure-temperature measurements of the speed of sound (an indirect route to obtain all of the observable thermodynamic properties of a fluid phase) as they must be carried out outside of the relaxation regions.[6-8] Furthermore, knowledge of ultrasound absorption is necessary in some methods used for the study of the nonlinear acoustic properties of the liquids.[9]

Unfortunately, there is a lack of ultrasound absorption in ILs data available in the literature. Apart from abovementioned studies using acoustic technique,[1-4] only two papers were published using an optic method, to date.[10,11] ILs are currently defined as molten salts with a melting temperature below 373 K. Simultaneously, salts that are liquid at room temperature form a subclass of ILs called room temperature ionic liquids (RTILs).[12,13] To the best of our knowledge, the available literature data on the ultrasound absorption are limited to only RTILs in practice. Apart from our previously reported results for 1-ethyl-3-methylimidazolium and 1-octyl-3-methylimidazolium bis(trifluoromethylsulfonyl)imides ($[C_2mim][NTf_2]$ and $[C_8mim][NTf_2]$) [2] as well as bis(1-ethyl-3-methylimidazolium)

tetrathiocyanocobaltate and bis(1-butyl-3-methylimidazolium) tetrathiocyanocobaltate ($[C_2mim]_2[Co(NCS)_4]$ and $[C_4mim]_2[Co(NCS)_4]$),[1] only two other research groups reported data obtained by means of a direct method based on the first travel pulse with a variable path length.[3,4] For example, Makino et al.[3] reported data for four imidazolium-based RTILs in the temperature range of (293-393) K but at three similar frequencies (e.g. 11.3, 34.9, and 57.7 MHz), whereas Mirzaev and Kaatze [4] studied ultrasound absorption of the ethylammonium nitrate (EAN) only isothermally (313.15 K) in the frequency range from 0.2 to 15 MHz. Using a transient grating (TG) method,[14] additional experimental results have been reported by Frez et al.[10] (for seven RTILs) and Kozlov et al.[11] (for four RTILs). Unfortunately, in both cases measurements have been carried out only at single frequency at 296.85 K or 301 K, respectively. Generally, the TG method seems more suitable for measuring ultrasound velocity than the ultrasound absorption, and in the case of RTILs, a few suchlike reports can be found.[15-19]

The abovementioned study of the ultrasound absorption and the recently observed non-Newtonian behavior along with lack of the dynamic crossover in the range of 1.2-1.5 T_g for $[C_nmim]_2[Co(NCS)_4]$ (n = 2,4) [1] have been the motivation for a more detailed analysis of the role of the elongation of the alkylside chain length in imidazolium cations on the molecular dynamics by a study of the ultrasound absorption and related properties for four consecutive (1-propyl-, 1-butyl-, 1-pentyl-, and 1-hexyl-) 1-alkyl-3-methylimidazolium bis(trifluoromethylsulfonyl)imides, i.e., $[C_nmim][NTf_2]$ (n = 3,4,5,6). $[C_nmim][NTf_2]$ are hydrophobic RTILs that contain a large hydrolytically-stable anion and these RTILs are representative of a broad group of aprotic ILs. Worthy of note is that $[C_6mim][NTf_2]$ is the reference substance recommended by IUPAC [20] and broadening its available property values as well as deeper knowledge about molecular dynamics may be additionally interesting to the research community. To complete the ultrasound absorption study and to obtain a set of

consistent data, the speed of sound, density, and kinematic viscosity were measured as well. From the measurement results, the ultrasonic relaxation spectra, the differences between the experimental absorption and the classical absorption, the relaxation strengths, the ratios of volume and shear viscosity, as well as, ultrasound velocity dispersion were calculated and analyzed in terms of differences in the length of the alkyl side chain of the imidazolium ring, together with the previously reported results for two other homologues of $[C_n\text{mim}][NTf_2]$ with (n = 2,8) [2] as well as $[C_n\text{mim}]_2[Co(NCS)_4]$ (n = 2,4).[1] The results were compared with the behavior of imidazolium based RTILs with hexafluorophosphate $[PF_6]^-$ anion, i.e., $[C_n\text{mim}][PF_6]$ (n = 4,6,8) as well as $[C_4\text{mim}][NTf_2]$ reported by Makino et al.[3]

In this work the speed of sound c_o is defined as the independent on frequency low-frequency limit of the phase ultrasound velocity for longitudinal-waves, whereas the term ultrasound velocity c is used in the case of the dependent on frequency phase ultrasound velocity for longitudinal-waves.

2. EXPERIMENTAL SECTION

2.1. Chemicals. The RTILs used in this work were purchased from QUILL Research Centre/School of Chemistry and Chemical Engineering, Queen's University of Belfast. The liquids were synthesized and purified according to known procedures.[21] The liquids were stored under argon, and the water content (< 200 ppm) was determined using the Karl Fischer method. Halide content was undeterminable by $AgNO_3$ testing; below the limit. Details about the synthesis, purification, and storage are given in the Supporting Information together with CAS numbers, molar mass M, cations and anion structures (Table S1 and Figure S1 of the Supporting Information).

2.2. Experimental systems. In this work, both the ultrasound absorption and speed of sound were measured by means of the so-called narrow-band technique. The ultrasound

absorption measurements were carried out using a measuring set based on the standard pulse method with a variable path length. There are absolute measurements of the absorption coefficient α by variation of the sample thickness, where the α values are obtained from the slope of the straight line (amplitude of the received pulses versus sample thickness). The measurements within the frequency range (10 to 300) MHz were executed using two sets of broadband ultrasonic heads ($LiNbO_3$ transducers) mainly at the temperature range of (293.15-323.15) K and at atmospheric pressure. During the measurements, the temperature of the sample was maintained in each case with an uncertainty ±0.05 K and the measuring cell was filled with argon to avoid contact of the sample with air (hygroscopic nature of the samples). The uncertainty of the α/f^{-2} data was estimated to be of ±2.5%. More details concerning the design and construction of the measuring set and the measurements procedure have been reported previously.[22,23]

The supplementary speed of sound measurements were carried out using a pulse-echo-overlap method. Our own measuring set (transmitting-receiving transducer with an acoustic mirror) operating at a fixed frequency of 2 MHz was used. For the calibration of the acoustic cell, redistilled and freshly degassed by boiling water (electrolytic conductivity 10^{-4} $S \cdot m^{-1}$) was used. During all measurements, the temperature of the sample was maintained by a cascade thermostat unit with fluctuations not exceeding ±0.05 K. The speed of sound measurements were done in a similar temperature range as in the case of ultrasound absorption. The uncertainty of the measured speeds of sound was estimated to be ±0.5 $m \cdot s^{-1}$. More details about the measuring set and method can be found elsewhere.[24,25]

The densities were measured with an Anton Paar DMA 5000 vibrating-tube densimeter, whereas the kinematic viscosities were measured using a pre-calibrated Ubbelohde viscometers from Schott. The densimeter was calibrated with water and dry air. The densities were measured over a range of temperature of 70 K or more (up to 363.15 K), and in each

case, the viscosity correction was made. For the kinematic viscosities, the measurements were done over a range of temperature of 40 K (from ca. 293 K to 333 K), and, if necessary, the Hagenbach correction for kinematic energy was applied. The temperature was maintained similar to those in the case of the speed of sound measurements, i.e., by a cascade thermostat unit with fluctuations not exceeding ±0.05 K. The uncertainty of the measured densities was ±0.05 kg·m^{-3}. In turn, the uncertainty of viscosity was ±1%.

During all experiments, temperature was determined according to ITS-90. Apart from the density measurements, temperature was determined using a certified Pt 100 probe and a digital Ertco-Hart thermometer.

3. MEASUREMENT RESULTS AND CALCULATIONS

3.1. Speed of Sound and Density. The experimental speed of sound and density values (Tables S2 and S3 of the Supporting Information) were approximated by the polynomials in the form:

$$Y(T) = \sum_{i=0}^{i=2} a_i \cdot (T - 293.15)^i \qquad (1)$$

where Y denotes density ρ or speed of sound c_o. The coefficients a_i determined by the unweighted least-squares method are reported in Table 1. It also appears that the values of the mean standard deviations from regression lines δ (residual deviations as well) are relatively small. In consequence, the values estimated from the regression functions are equal to the raw data within the limits of the measurements' repeatability.

Table 1

Values of the Coefficients, a_i of the Eq 1 Together with the Mean Standard Deviations δ from the Regression Line for the Temperature Dependence of the Speed of Sound c_o and Density ρ for the Investigated RTILs

	a_0	a_1	a_2	δ[a]
		[C_3mim][NTf_2]		
c_o /m·s^{-1}	1241.58	-2.2627	$2.778\cdot10^{-3}$	0.02
ρ /kg·m^{-3}	1479.965	-0.991161	$3.4497\cdot10^{-4}$	0.003
		[C_4mim][NTf_2]		
c_o /m·s^{-1}	1237.19	-2.2460	$2.577\cdot10^{-3}$	0.02
ρ /kg·m^{-3}	1441.141	-0.961018	$3.0567\cdot10^{-4}$	0.007
		[C_5mim][NTf_2]		
c_o /m·s^{-1}	1237.70	-2.2864	$2.523\cdot10^{-3}$	0.02
ρ /kg·m^{-3}	1406.885	-0.936744	2.1829	0.008
		[C_6mim][NTf_2]		
c_o /m·s^{-1}	1237.14	-2.3131	$2.548\cdot10^{-3}$	0.01
ρ /kg·m^{-3}	1376.496	-0.920634	$2.6281\cdot10^{-4}$	0.005

[a] $\delta = (\sum_{i=1}^{n}(y_{i,\exp} - y_{i,calc})^2/(n-m))^{1/2}$ where n is the number of experimental points, m is the number of fitted coefficients, and y denotes c_o or ρ.

3.2. Viscosity. Kinematic viscosities v measured mainly in the temperature range (293-333) K are summarized in Table S4 of the Supporting Information. Obtained as product $\rho\cdot v$,

the dynamic viscosities at low shear rates (static shear viscosities) were approximated as a function of the temperature by the use of an equation in the form:

$$\eta_s = A' \cdot \exp(B' \cdot (T - T_0)^{-1}) \quad (2)$$

This is the Vogel-Fulcher-Tamman (VFT) equation, where T_0 is an ideal glass transition temperature. The estimated (unweighted least-squares) coefficients (A', B', and T_0) are reported in Table 2 along with the standard mean deviation δ from the regression line (η_s values are listed in Table S4). The existing correlation between the VFT B' and T_0 coefficients is common in classifying glass-forming liquids.[26,27] It appears that the obtained ratios B'/T_0 are small, i.e., in each studied case, $B'/T_0 < 10$ (Table 2). This corresponds with *fragile* glass-forming materials, which show large deviations from the Arrhenius law.[27,28]

Table 2

VFT Equation (Eq 2) Coefficients, Standard Mean Deviations δ [a], and Ratios B'/T_0 for Measured RTILs.

A' / mPa·s	B' / K	T_0/ K	B'/T_0	δ[a]/ mPa·s
		[C_3mim][NTf_2]		
0.2040	686.2	171.15	4.0	0.002
		[C_4mim][NTf_2]		
0.2306	668.7	173.15	3.9	0.01
		[C_5mim][NTf_2]		
0.3168	589.9	185.15	3.2	0.032
		[C_6mim][NTf_2]		
0.2300	680.3	179.15	3.8	0.011

[a] See footnote in Table 1.

3.3. Ultrasound Absorption. For the RTILs studied, the ultrasound absorption coefficients of α per squared frequency f, i.e., the quotients α/f^{-2} are plotted against $\log f$ in Figures 1-4 and the raw data are summarized in Table S5 of the Supporting Information. It appears that within the investigated frequency range, the clear dependence of the quotient α/f^{-2} on frequency is observed for all samples at each temperature. At the same time, the variable dependence of α/f^{-2} on T at a constant frequency is visible.

To represent the quotients α/f^{-2} *versus* frequency, the following function was applied:

$$\alpha \cdot f^{-2} = A \cdot (1 + (f \cdot f_{rel}^{-1})^2)^{-1} + B \quad (3)$$

where A is the relaxation amplitude, f_{rel} is the relaxation frequency of the discrete single Debye relaxation process, and B denotes the sum of the classical part of the absorption and the contributions from possible processes with relaxation frequencies much higher than f_{rel}. The A, B and f_{rel} values are estimated by the least-squares method and are shown in Table 3 along with the relaxation times τ_{rel} ($\tau_{rel} = (2 \cdot \pi \cdot f_{rel})^{-1}$) and the relaxation strengths r. The relaxation strengths were calculated from:

$$r = A \cdot c_o \cdot (2 \cdot \pi^2 \cdot \tau_{rel})^{-1} \quad (4)$$

where c_o is the speed of sound at 2 MHz (i.e., ultrasonic velocity in the low frequency limit).

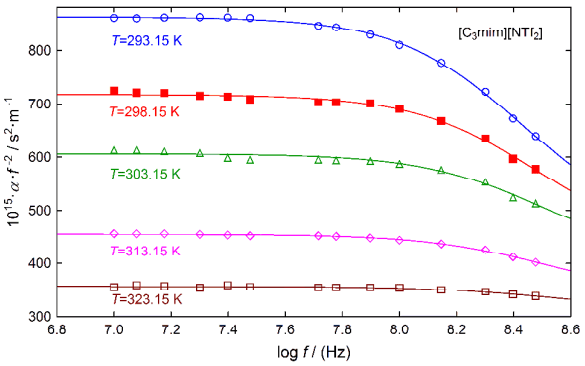

Figure 1. The ultrasound absorption coefficient per squared frequency α/f^{-2} plotted against $\log f$ for $[C_3mim][NTf_2]$ at temperatures: ○, 293.15 K; ■, 298.15 K; Δ, 303.15 K; ◊, 313.15 K; and □, 323.15 K. The solid lines represent fitted relaxation functions.

Table 3

Coefficients of the Relaxation Equation (Eq 3) Together with Standard Mean Deviation δ [a] and Relaxation Strength r (Eq 4) for [$C_n$mim][NTf_2] Studied at Ambient Pressure and Temperatures T.

T/ K	$10^{15}\cdot B$ / $m^{-1}\cdot s^2$	$10^{15}\cdot A$ / $m^{-1}\cdot s^2$	f_{rel} / MHz	$10^{15}\cdot\delta$ [a] / $m^{-1}\cdot s^2$	$10^2\cdot r$
		[C_3mim][NTf_2]			
293.15	458.2	403.9	270	2.6	4.31
298.15	432.6	285.3	301	4.7	3.36
303.15	404.1	201.8	320	5.7	2.51
313.15	338.4	116.2	330	1.2	1.46
323.15	314.1	42.3	339	1.5	0.54
		[C_4mim][NTf_2]			
283.15	572.7	901.0	182	11	6.58
293.15	487.0	529.7	251	3.4	5.24
298.15	439.2	403.4	289	3.9	4.55
303.15	418.3	281.0	311	3.0	3.38
313.15	398.2	124.1	325	0.9	1.53
323.15	359.9	45.3	333	2.7	0.56
		[C_5mim][NTf_2]			
288.15	602.9	967.7	169	15	6.50
293.15	535.6	732.0	211	8.7	6.08
298.15	449.1	595.3	256	4.9	5.95
303.15	409.2	446.7	295	5.3	5.10
313.15	410.6	209.2	311	2.4	2.47

323.15	388.6	92.4	327	1.1	1.13
		[C_6mim][NTf_2]			
293.15	568.2	938.1	172	6.7	6.35
298.15	475.6	770.3	210	5.6	6.30
303.15	458.1	559.2	238	4.9	5.14
313.15	447.3	291.3	245	3.7	2.71
323.15	415.5	143.1	260	3.4	1.39

[a] See footnote in Table 1.

A classical part of the absorption, i.e., a classical absorption coefficient per squared frequency α_{cl}/f^{-2}, can be calculated from the formula:

$$\alpha_{cl} \cdot f^{-2} = 8 \cdot \pi^2 \cdot \eta_s \cdot (3 \cdot \rho \cdot c_o^3)^{-1}, \quad (5)$$

where η_s is the static shear (Newtonian) viscosity (i.e., the shear viscosity with a shear rate ≈ 0: in other words, η_s for $2 \cdot \pi \cdot f \rightarrow 0$), and ρ is the density. The obtained values of α_{cl}/f^{-2} are summarized in Table 4. It should be noted that shown by Kirchhoff an additional energy dissipation caused by a finite coefficient of heat conduction λ can be here neglected because for most liquids (excluding liquid metals), this contribution (so-called Kirchhof term) is very small in comparison to the value calculated only on the base of the viscosity (Stokes term) (eq 5). For the calculations, the values of densities, speeds of sound, and static shear viscosities measured in this work were used.

To represent the α/f^{-2} dependence on T at a constant frequency, an Arrhenius type formula was used in the form:

$$\ln(\alpha \cdot f^{-2}) = \ln A_\alpha + E_\alpha \cdot (RT)^{-1} \quad (6)$$

where E_α is the activation energy, and A_α is a pre-exponential constant. The calculated values of E_α and A_α at chosen frequencies are summarized in Table S6 of the Supporting Information.

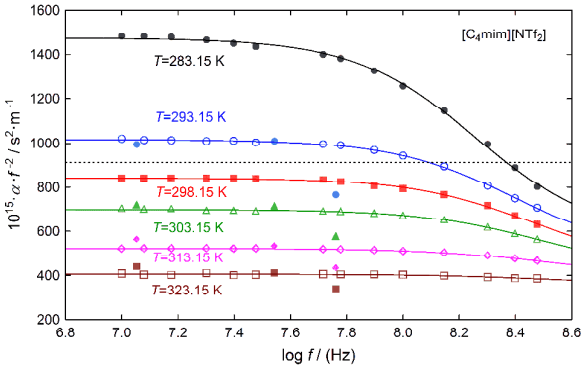

Figure 2. The ultrasound absorption coefficient per squared frequency $\alpha \cdot f^{-2}$ plotted against $\log f$ for $[C_4mim][NTf_2]$ at temperatures: black ●, 283.15 K; blue ○, 293.15 K; red ■, 298.15 K; green Δ, 303.15 K; pink ◊, 313.15 K; and brown □, 323.15 K. For comparison, data from ref. 3 are included: blue ●, 293.15 K; green ▲, 303.15 K; pink ♦, 313.15 K; and brown ■, 323.15 K. The solid lines represent fitted relaxation functions. The dashed black line indicates the classic absorption contribution according to eq 5 at temperature 283.15 K.

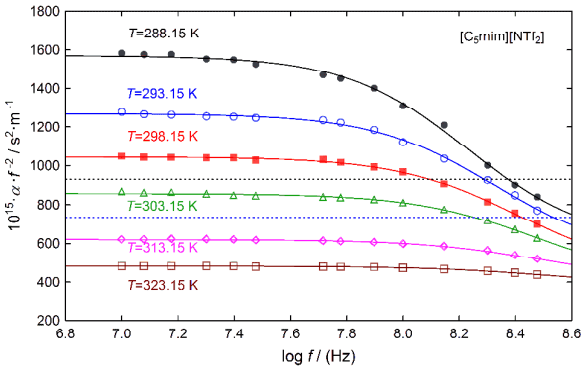

Figure 3. The ultrasound absorption coefficient per squared frequency $\alpha \cdot f^{-2}$ plotted against $\log f$ for $[C_5mim][NTf_2]$ at temperatures: ●, 288.15 K; ○, 293.15 K; ■, 298.15 K; Δ, 303.15 K; ◊, 313.15 K; and □, 323.15 K. The solid lines represent fitted relaxation functions. The dashed

lines (sequence as above) indicate the classic absorption contributions according to eq 5 at temperatures 288.15 K (black) and 293.5 K (blue).

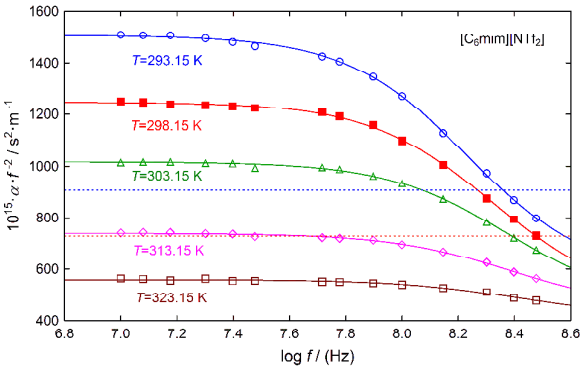

Figure 4. The ultrasound absorption coefficient per squared frequency $\alpha \cdot f^{-2}$ plotted against log f for $[C_6mim][NTf_2]$ at temperatures: ○, 293.15 K; ■, 298.15 K; Δ, 303.15 K; ◊, 313.15 K; and □, 323.15 K. The solid lines represent fitted relaxation functions. The dashed lines (sequence as above) indicate the classic absorption contributions according to eq 5 at temperatures 293.15 K (blue) and 298.5 K (red).

4. DISCUSSION

4.1. Speed of Sound, Density, and Viscosity. As expected, both density and viscosity decreased with the increasing temperature in a linear and an exponential manner, respectively. Both the density and the viscosity of the RTILs studied clearly changed with the elongation of the side alkyl chain in the 3-methylimidazolium ring of the cation, i.e., the longer the alkyl chain, the smaller density and higher viscosity.

The speed of sound decreased with the increasing temperature (negative temperature coefficient) also near linearly, i.e., the behavior is also typical. However, contrary to many other quantities, c_o is not a distinguishing feature for RTILs tested. Only small (e.g., c_o in $[C_4mim][NTf_2]$ and $[C_6mim][NTf_2]$ at 298.15 K differs only by amounts 0.5 $m \cdot s^{-1}$) and somewhat peculiar changes with the elongation of the alkyl chain in the 3-

methylmimidazolium ring of cation are observed. Considering the c_o values for $[C_2mim][NTf_2]$ and $[C_8mim][NTf_2]$ reported previously,[2] it is clear (Figure 5) that the variation of c_o is rather unusual, having a minimum value most probably for $[C_5mim][NTf_2]$; non-monotonic changes of c_o with the elongation of the alkyl chain length in cations of $[C_nmim][NTf_2]$ were already mentioned earlier.[2,29]

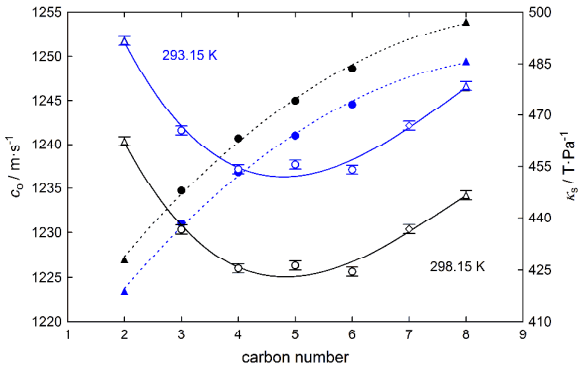

Figure 5. The speed of sound c_o (open symbols) and isentropic compressibility coefficient κ_S (filled symbols) plotted against carbon number in side alkyl chain of 3-methylimidazolium ring of $[C_nmim][NTf_2]$ at temperatures of 293.15 K (blue symbols) and 298.15 K (black symbols) for carbons number: (Δ,▲), 2 and 8, data from ref 2; (○,●), 3, 4, 5,and 6, this work; and ◊, 7, unpublished data. Uncertainty bars ± 0.5 m·s^{-1}. Lines arbitrary (c_o, continuous; κ_S, dashed).

Few available literature data on the speed of sound in ILs under study exist. According to our best knowledge, only two papers reported c_o in $[C_3mim][NTf_2]$,[21,30] eight in $[C_4mim][NTf_2]$,[2,3,10,18,17,21,31,32] and four in $[C_6mim][NTf_2]$.[10,33-35] Moreover, in the case of $[C_5mim][NTf_2]$, only one isothermal value is available to date.[10] Generally, it appears that the agreement between the values determined in this study and the values reported in the literature is acceptable (Figure 6). With the exception of the isothermal data of Demizu et al.[17] and Fukuda et al.[18] (not shown in the figure because the values obtained by the use of TG

method show very high deviations of -0.7 % (313 K) and 1.6 % (298.15 K), respectively), in practice, the majority of the data deviates less than ±0.2 % (Figure 6). However, it should be noted that various techniques have been used, which are sometimes not specially suitable for the accurate speed of sound measurements.[3,10,18,17] Simultaneously, the ILs are in general difficult objects for speed of sound measurements. First of all, their purity, hygroscopic nature, high viscosity and high ultrasound absorption create problems, which are unfortunately most often ignored.

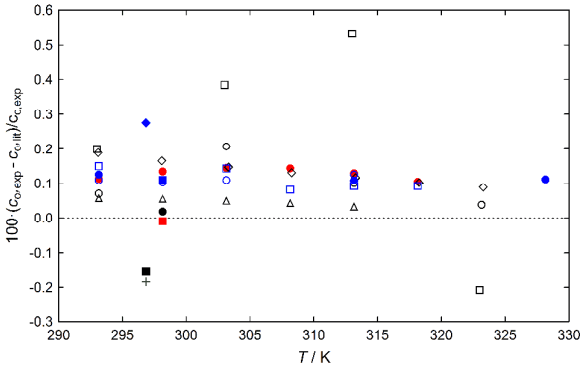

Figure 6. Deviations between the literature values $c_{o,lit}$ and this work's experimental values $c_{o,exp}$ plotted as $100\cdot(c_{o,lit}-c_{o,exp})/c_{o,exp}$ against temperature T for: (i) $[C_3mim][NTf_2]$; red ●, ref 30; and red ■, ref 21: (ii) $[C_4mim][NTf_2]$: black ◊, ref 2; black, □, ref 3; black ■, ref 10; black ●, ref 21; black ○, ref 31; and black Δ, ref 32; (iii) $[C_5mim][NTf_2]$; green +, ref 10: (iv) $[C_6mim][NTf_2]$; blue ♦, ref 10; blue □, ref 33; blue,●, ref 34; and blue ○, ref 35.

Taking into account that the measurement of c_o is only one way to obtain isentropic compressibility, we calculated the isentropic compressibility coefficient κ_S and its molar counterpart K_S as follows:

$$\kappa_S = (\rho \cdot c_o^2)^{-1} \quad (7)$$

$$K_S = \kappa_S \cdot M \cdot \rho^{-1} \quad (8)$$

The calculated values of κ_S and K_S at the chosen temperatures are summarized in Table S7 of the Supporting Information. In all cases, in contrast to c_o, we observed an increase of compressibility with the increasing temperature as well as an increase of compressibility from $[C_3mim][NTf_2]$ to $[C_6mim][NTf_2]$ (Figure 5). The compressibility is generally rather moderate (similar as for associating molecular liquids); however, they are higher than in the case of adequate imidazolium-based RTILs containing ethylsulfate $[EtSO_4]^-$ and trifluoromethanesulfonate $[TfO]^-$ anions.[2] Thus, the higher compressibility could be related to the structure and size of the $[NTf_2]^-$ anion.

4.2. Ultrasound absorption. As mentioned in Section 3.3, within the investigated frequency and temperature range, the quotient $\alpha \cdot f^{-2}$ is dependent both on frequency and temperature in all cases (Figures 1-4). In other words, in each case, the relation $d(\alpha \cdot f^{-2})/df < 0$ and $d(\alpha \cdot f^{-2})/dT < 0$ is observed. Thus, the alkyl chain length in the imidazolium cation causes clear differences in the ultrasound absorption spectra of the RTILs investigated (see Figure 7). Firstly, as the alkyl chain length increases, the relaxation regions shift towards lower frequencies. Secondly, the magnitude of the quotient $\alpha \cdot f^{-2}$ increases in the order: $[C_3mim][NTf_2] < [C_4mim][NTf_2] < [C_5mim][NTf_2] < [C_6mim][NTf_2]$, i.e., from middle absorbing $[C_3mim][NTf_2]$ to rather highly absorbing $[C_6mim][NTf_2]$ (the frequency of normalized absorption at $T = 298.15$ K and $f = 10$ MHz is $(725.4 \cdot 10^{-15}$ and $1249 \cdot 10^{-15})$ $m^{-1} \cdot s^2$, respectively). The obtained results are fully consistent with the literature results reported for $[C_2mim][NTf_2]$ [2] and $[C_8mim][NTf_2]$ [2] (Figure 7), and generally, the behavior of $[C_nmim][NTf_2]$ can be related to the increase of the nonpolar part of the cation. At the same time, the clear increase of $\alpha \cdot f^{-2}$ with the lengthening of the hydrocarbon chain length in the imidazolium cation observed is contradictory to conclusion of Frez et al.[10] that the cation exerts no significant effect. Evidently, this conclusion was a consequence of the uncertainty of the measuring method used, i.e., TG. Moreover, without doubt, $\alpha \cdot f^{-2}$ in the non-relaxation

region below the relaxation frequency is controlled by viscosity and simultaneously, none of the obtained spectra reaches a frequency independent *B* value.

Because of the very limited literature data, a direct comparison is not possible in practice; however, a comparison with the fragmentary data (at three frequencies only) for [C_4mim][NTf_2], which was reported by Makino et al.,[3] shows differences (Figure 2). The αf^{-2} values obtained in this work are consistent with results given by Makino et al. at 11.3 and 37.7 MHz within the declared uncertainties, while values at 57.7 MHz (the highest frequency of their measurement range) have a very poor agreement with our results. They are significantly lower than those obtained in this study. Consequently, the data of Makino et al. clearly indicate the relaxation region at lower frequencies in comparison with our results. This disagreement could be connected to a systematic error in relation to the measurements at 57.7 MHz (fifth-harmonic of the used transducers). In the case of the remaining RTILs, the lack of the literature data makes any comparison impossible.

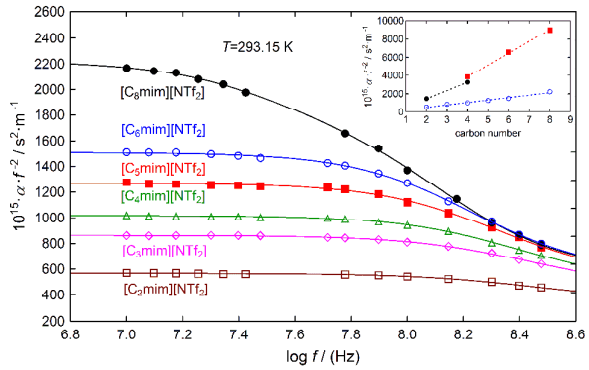

Figure 7. The ultrasound absorption coefficient per squared frequency $\alpha \cdot f^{-2}$ plotted against log *f* at temperature 293.15 K for: □, [C_2mim][NTf_2], ref 2; ◊, [C_3mim][NTf_2]; Δ, [C_4mim][NTf_2]; ■, [C_5mim][NTf_2]; ○ [C_6mim][NTf_2]; and ●, [C_8mim][NTf_2]. In the last case, data from ref 2 are fitted again by the use of model with two Debye terms (Table S8). The solid lines represent fitted relaxation functions. The inset shows the $\alpha \cdot f^{-2}$ values in the non-relaxation region plotted against carbon number in side alkyl chain of 3-methylimidazolium

ring for: blue ○, $[C_n mim][NTf_2]$; red ■, $[C_n mim][PF_6]$ (data at 11.3 MHz from ref 3); and black ●, $[C_n mim]_2[Co(NCS)_4]$. Broken lines arbitrary.

It is interesting that for the $[C_n mim][NTf_2]$ measured in this study (n = 3,4,5,6) and reported previously (n = 2,8),[2] $\alpha \cdot f^{-2}$ in the non-relaxation region below the relaxation frequency increases almost linearly with the increasing number of methylene groups in the alkyl chain of the imidazolium cation (inset in Figure 7). Thus, the $\alpha \cdot f^{-2}$ shows an additive character here. Similar behavior can be roughly observed in the case of $[C_n mim][PF_6]$ (n = 4,6,8) (inset in Figure 7). Thus, it seems that the above-mentioned linearity between the values of $\alpha \cdot f^{-2}$ in this non-relaxation region and the length of the alkyl side chain of the cationic imidazolium ring is anion independent; however, the magnitude of this effect (slope) is clearly anion dependent, and in the case of smaller and more globular $[PF_6]^-$ anion, it is much greater in comparison to a much larger non-globular $[NTf_2]^-$ anion. Simultaneously, evidently lower absorption is observed for the $[NTf_2]^-$ anion in comparison with the $[PF_6]^-$ anion. Anion dependents are also relaxation regions as a comparison of the ultrasound absorption spectra for imidazolium RTILs with an $[NTf_2]^-$ anion (Figure 7) and a $[PF_6]^-$ anion (reported in ref. 3) with same carbon chain lengths in the cation leads to the conclusion that the presence of the $[PF_6]^-$ anion moves the relaxation region towards lower frequencies. Interestingly, both anions are halogenated and contain fluorine, but the $[PF_6]^-$ anion is octahedral, relatively small, and more globular, whereas $[NTf_2]^-$ is a nonglobular relatively large anion with the possibility of the internal rotations about the two S-N bonds (Figure S1). These rotations (clarified both theoretically [36] and experimentally [37]) are a reason of a large internal flexibility of the anion, and its flexible nature is reflected in the occurrence of two equilibrium structures: cis and trans.

At the same time, the activation energy (calculated by the use of eq 6) of the dissipative processes related to ultrasound absorption decreases with the increasing frequency for each RTIL studied (Table S6). Interestingly, however, for frequencies below ca.140 MHz E_α increases from [C_3mim][NTf_2] to [C_6mim][NTf_2], whereas for higher frequencies an inverse trend is observed, i.e., E_α decreases from [C_3mim][NTf_2] to [C_6mim][NTf_2]. Thus, at frequency in the vicinity of 140 MHz E_α is the same for each RTIL studied.

Generally, the obtained ultrasonic spectra can be discussed assuming aggregation processes determined by Coulomb forces and dispersion forces as well as hydrogen bonding. The hydrogen-bonding contribution to the overall interaction energy in aprotic ILs is today widely accepted and well documented among others using far infrared and terahertz spectroscopy (FIR and THZ) studies,[38-40] and although such contribution is only about 10 %, the nature of hydrogen-bond interactions (e.g., directional) can significantly influence the properties of such ILs. Generally, ILs can be treated as structured solvents (from ion pairs, ion clusters to H-bonded networks, micelle-like and bi-continuous structures).[13] The first suggestion of a bi-continuous structure considered to include polar and nonpolar regions was introduced by Schröder et al.[41] Today, it is well established that the polar domains are not homogeneously distributed but form a continuous 3D polar network.[13] These polar networks coexisted with nonpolar domains. However, in the case of short alkyl groups in imidazolium cations, small and globular nonpolar domains form within the polar network. In turn, when the alkyl chain length increases, the nonpolar domains interconnect in a bi-continuous sponge-like nanostructure. According to Canongia Lopes,[42] this progression seems to be marked by the butyl side chain. Thus, assuming that aprotic RTILs studied can be treated as a mixture of polar and nonpolar domains, ultrasonic relaxation based on an equilibrium between these domains can be described by the discrete relaxation time according to eq 2 (i.e., by a single Debye-type relaxation term). The dynamics of the domain structure of ILs was recently

investigated by Kofu et al. [43] using the neutron spin echo spectroscopy (NSE). Data obtained using this technique, which is also able to investigate microscopic motions, show that the relaxation mechanism is most probably more complicated and cannot be assigned solely to the domain dynamics. This has been demonstrated by comparison of the shear viscosity relaxation and NSE results, which implies that the shear viscosity relaxation cannot be explained solely by the domain or microscopic structures.[44]

An analysis of the relaxation strengths (dependent on the enthalpy ΔH and volume ΔV change connected to the process disturbed by the acoustic wave) shows that the greatest r values are observed in the case of $[C_6mim][NTf_2]$ (Table 3). This finding is not surprising taking into account that $[C_6mim][NTf_2]$ shows highest compressibility (reflects volume changes in relation to pressure) and isobaric heat capacity (reflects enthalpy changes in relation to temperature) from the four RTILs studied (Table S5 and ref.45). Generally, the relaxation strength increases with increasing the alkyl chain length of the cation, but increments decrease.

Although the obtained spectra in principle are satisfactorily described using a single Debye type exponential function of time, inspection of all fitting results summarized in Table 3 shows that the higher absorption the poorer the fitting. A similar situation, i.e., the higher absorption the poorer fitting by the single Debye model, was also observed in the case of $[C_8mim][NTf_2]$.[2] Very recently a similar problem was observed in the case of highly absorbing paramagnetic $[C_2mim]_2[Co(NCS)_4]$ and $[C_4mim]_2[Co(NCS)_4]$, where the single Debye model completely failed,[1] and the fitting with a stretched function was discussed by the authors. The symmetrical Cole-Cole function was used with a parameter of α_{cc} ($0 < \alpha_{cc} < 1$), which reflects the distribution of relaxation times (the smaller the α_{cc}, the wider the distribution, and if $\alpha_{cc} = 1$, this model is reduced to the Debye model with a single relaxation term (eq 2)); however, the fitting gave α_{cc} (from 0.78 to 0.89), indicating small distributions

of relaxation time. However, because symmetrical shape of the spectra seems somewhat puzzling, and results for the background absorption at frequencies far above the experimental range are inconsistent, we again fitted the data reported in ref 1 by the use of a model with two Debye-type relaxation terms. The same model is also used for refitting the data reported in ref 2 for $[C_8mim][NTf_2]$. The results are summarized in Table S8 of the Supporting Information. Summing up, it appears that the model with two Debye relaxation times is the most appropriate description for the spectra of $[C_8mim][NTf_2]$, $[C_2mim]_2[Co(NCS)_4]$ and $[C_4mim]_2[Co(NCS)_4]$. This solution ensures the consistency of all results and is plausible because in each of the abovementioned three cases obtained relaxation frequencies associated with the two coupled processes differs sufficiently from each other to separate the contributions to the absorption spectrum from two processes. Generally, the relaxation function can be made up of two (or more) parts only when the ratio of the relaxation times fulfills the inequality $\tau_1/\tau_2 > 4$ and the ratio of the relaxation amplitudes fulfills condition $0.25 < A_2/A_1 < 4$.[46] When these conditions are not fulfilled, it may be impossible to resolve the contributions to the absorption spectrum from two processes (e.g., similar relaxation times), and the absorption data will have the appearance of a single relaxation curve. In principle, however, even the fact that the absorption data fit a single relaxation curve does not necessarily mean that there is in fact a single relaxation process.

It should be noted here that apart from the traditional way of interpreting ultrasound absorption data, for theories of ultrasound absorption in liquids progress is very weak in practice. Indeed, an interesting statistical-mechanical theory for the description of ultrasound absorption in liquids on a microscopic level has been presented by Kobryn and Hirata,[47] but its application in a real system remains a subject of future works.

Although a direct comparison of the obtained ultrasound absorption spectra was not possible, the comparison with the ultrasound velocity dispersion reported by Fukuda et al.[18]

for $[C_4mim][NTf_2]$ at 298.15 K shows some agreement, at least qualitative. According to Fukuda et al., [18] the ultrasound velocities are constant below 260 MHz within an experimental error, i.e, below 260 MHz the frequency dependence was not observed and a low-frequency limit of the ultrasound velocity (i.e., the c_o value) was attained. The ultrasound velocity dispersion calculations done by the use of a simple viscoelastic Maxwell model show some consistency but only at frequencies below 400 MHz,[3] which is not especially surprising taking into account used model. In turn, according to simple Debye model used in this work for description of the ultrasound absorption data for $[C_4mim][NTf_2]$ at 298.15 K, the relaxation frequency lies at 289 MHz. Thus, the results obtained by the use of different techniques are only consistent to a certain degree . As shown in Figure 8, the estimated dispersion curve for $[C_4mim][NTf_2]$ indicates velocity dispersion at significantly lower frequencies than 260 MHz. A comparison between ultrasound velocity dispersion reproduction with the simple Debye model and previously reported in the literature dielectric relaxation[48] led Fukuda et al.[18] to conclude that in the case of $[C_4mim][NTf_2]$ structural relaxation is much faster than re-orientation relaxation, i.e., the relaxation is decoupled. On the other hand, both relaxations were strongly coupled in the case of $[C_4mim][PF_6]$. Fukuda et al.[18] interpreted this difference as a result of the different anion structures.

The obtained values of background absorption B for the highest investigated temperatures indicate that other relaxation processes can be present in the higher frequency range (B values are higher than values obtained by eq 5). On the other hand a clear indication of the non-Newtonian behavior is observed. Apart from $[C_3mim][NTf_2]$, for remaining three measured $[C_nmim][NTf_2]$, the α/f^{-2} values at lowest temperatures are in each case above frequencies about 230 MHz (Figures 2-4) smaller than those obtained by the Stokes relation (eq 5). This means that a shear viscosity relaxation in the MHz range is present, and the frequency dependence of α/f^{-2} can also be closely connected with a relaxation behavior of the shear

viscosity, i.e., in the considered frequency range the shear viscosity must decrease with the increasing frequency. A similar behavior has been reported for $[C_8mim][NTf_2]$ where $\alpha < \alpha_{cl}$ was observed above ca. (150 and 180) MHz at temperatures of (293.15 and 298.15) K, respectively.[2] At similar temperatures and frequencies, $\alpha < \alpha_{cl}$ was also observed in the case of $[C_2mim]_2[Co(NCS)_4]$, whereas in the case of $[C_4mim]_2[Co(NCS)_4]$, lower frequencies (clearly below 100 MHz) were observed.[1] This type of behavior has been observed in the past at similar temperatures for molecular organic liquids as well;[23,49,50,55] however, it should be noted that a separate determination of the shear viscosity behavior requires a separate study of the shear ultrasound wave because ultrasound relaxation spectra determined using a longitudinal wave are not suitable to investigate the microscopic origin of the shear viscosity (there are difficulties in the separation of the contributions of volume and shear viscosities to the ultrasonic relaxation). It is a general agreement that, if $\alpha < \alpha_{cl}$, the shear viscosity relaxation must be present.[1,2,5,23,49,50,55] Assuming that the shear viscosity relaxation is present, and taking into account the simple Maxwell model, the real part $\eta'(\omega)$ of the complex (relaxing) shear viscosity can be expressed as:

$$\eta'(\omega) = \eta_S \cdot (1 + \omega^2 \tau_M^2)^{-1} \quad (9)$$

where $\omega = 2 \cdot \pi \cdot f$ and τ_M are the angular frequency and Maxwell relaxation time, respectively. The Maxwell relaxation time is defined as the ratio of η_S and the limiting shear modulus G_∞

$$\tau_M = \eta_S \cdot G_\infty^{-1} \quad (10)$$

Since the temperature variation of G_∞ is usually much smaller than that of η_S, the τ_M is approximately proportional to η_S. The larger increase η_S than the τ_M with the lengthening the alkyl chain in the imidazolium cation is interpreted as the decrease in G_∞ with the increase of the chain length.[51] The decrease in G_∞ is also connected with the decrease in the Walden

product and slight increase of the ratio of the shear viscosity and conductivity relaxation times τ_M and τ_Λ.[51]

According to Yamaguchi et al.,[52] the increase in the length of the alkyl chain of the cation for $[C_n mim][PF_6]$ (n = 4,6,8) leads to the lower-frequency shift of the shear relaxation frequency. At the same time, the shear relaxation frequency of $[C_4 mim][PF_6]$ also shifts to the lower frequency in comparison to $[C_4 mim][NTf_2]$, i.e., the shear relaxation times of these two RTILs are evidently different, and this difference is connected to differences in the anions. Thus, the present results obtained from ultrasound absorption are consistent with the results reported for shear relaxation.[52]

The values of the ratios α/α_{cl} in the non-dispersion region below the relaxation frequency (Table 4), along with the negative temperature coefficients of ultrasound absorption $\alpha^{-1}\cdot(d\alpha/dT)$, are typical for structural relaxation. From the ratio α/α_{cl}, the ratio η_v/η_s can be estimated from the following relationship:

$$\eta_v/\eta_s = 4/3\cdot(\alpha/\alpha_{cl}-1), \quad (11)$$

where η_v is the volume viscosity, which is a measure of the resistance of the liquid to a pure expansion or compression. It is worthy of notice that using the acoustic data is in practice the only way to determine the values of η_v, as they cannot be measured to date directly. The volume viscosity reflect the relaxation of both rotational and vibrational degrees of molecular freedom, whereas the shear viscosity reflect principally translational molecular motions as well as rotational motion through the translation-rotation coupling. The frequency independence of the η_v was suggested as a necessary condition for claiming that the liquid is Newtonian.[53] From this point of view, RTILs studied are obviously non-Newtonian.

Table 4

Classical Ultrasound Absorption α_{cl}/f^{-2}, the Ratios of the Observed [a] to the Classical

Absorption α/α_{cl}, the Temperature Coefficients of Absorption [a] $\alpha^{-1}\cdot(d\alpha/dT)$, and the Ratios of the Static Shear Viscosity to the Volume Viscosity [a] η_S/η_V for Measured RTILs at ambient Pressure and Temperatures T.

T/ K	$10^{15}\cdot\alpha_{cl}f^{-2}$ / $m^{-1}\cdot s^2$	α/α_{cl}	η_S/η_V	$10^2\cdot\alpha^{-1}\cdot(d\alpha/dT)$ / K^{-1}
		$[C_3mim][NTf_2]$		
293.15	525.4	1.650	0.866	-3.27
298.15	434.1	1.671	0.895	-3.36
303.15	364.7	1.680	0.907	-3.35
313.15	268.7	1.706	0.942	-2.77
323.15	207.7	1.730	0.973	-1.37
		$[C_4mim][NTf_2]$		
283.15	912.9	1.614	0.819	-3.40
293.15	585.1	1.738	0.984	-3.76
298.15	482.7	1.745	0.994	-3.83
303.15	405.1	1.726	0.968	-3.76
313.15	298.2	1.751	1.002	-2.75
323.15	230.2	1.760	1.013	-0.61
		$[C_5mim][NTf_2]$		
288.15	930.5	1.688	0.917	-3.90
293.15	736.3	1.721	0.962	-4.20
298.15	596.5	1.751	1.001	-4.34
303.15	493.2	1.736	0.981	-4.36
313.15	355.0	1.746	0.995	-3.46
323.5	270.3	1.780	1.040	-1.15
		$[C_6mim][NTf_2]$		

293.15	907.1	1.661	0.881	-3.61
298.15	728.3	1.711	0.947	-3.75
303.15	596.8	1.705	0.939	-3.83
313.15	421.8	1.751	1.001	-3.18
323.15	315.6	1.770	1.027	-1.43

[a] At frequencies below the relaxation region.

An inspection of Table 4 shows that the obtained η_v/η_s values are around 1, which is similar for many associated molecular liquids.[23] Thus, the magnitude of the η_v values is very close to the η_s values. Generally, if η_v/η_s is near 1 and approximately temperature independent (as in our case), it is well established for molecular liquids that a similar activation enthalpy for both viscosities can be supposed. Then, a similar scenario may be present in the case of the aprotic RTILs studied; however, the temperature dependence of η_v/η_s shows a small increasing trend. This trend is very weak but can suggested a small and increasing contribution from the aforementioned rotational relaxation process connected with the internal structures of anion. As known, in the case of isomeric rotational relaxation processes in molecular organic liquids, the η_v/η_s values are generally large and change with temperature changes.[54] Generally, the results obtained in this work (Table 4) are in excellent agreement with the η_v/η_s values extracted from the ultrasound absorption data reported earlier[2] for $[C_2mim][NTf_2]$ and $[C_8mim][NTf_2]$ because in the case of $[C_2mim][NTf_2]$, we obtained 0.873 and 0.852 at temperatures of (293.15 and 298.15) K, respectively, whereas in the case of $[C_8mim][NTf_2]$, we obtained 1.113 and 1.061, respectively. For three of four of the $[C_2mim]$-based RTILs with different anions investigated recently by Kozlov et al.[11] using a TG experiment, the η_v/η_s values are also in reasonable agreement. However, in the case of $[C_2mim][NTf_2]$, the value $\eta_v/\eta_s \approx 0$ (at 301 K) reported by Kozlov et al.[11] is contradictory to

the values (i.e., 0.873 and 0.852) extracted from a previous report.[2] It should be noted that an approach used to determine the bulk viscosity by means of a TG experiment "*may introduce a significant error*", as self-stated by Kozlov et al.[11]

4.3. Effect of ultrasound absorption on speed of sound. Ultrasound velocity and absorption are two fundamental propagating parameters of an ultrasound wave. In real liquids, the intensity of a longitudinal wave decreases exponentially when passing through a liquid. Thus, the dissipation of energy from the ultrasound wave is in practice always present (the classical absorption is present in all liquids); however, the effect of ultrasound absorption on the speed of sound may be ignored so long as $\alpha << \omega \cdot c_o^{-1}$ (or in a rearranged form so long as $\alpha \cdot c_o \cdot (2 \cdot \pi \cdot f)^{-1} << 1$). For instance, at 2 MHz and 298.15 K in water, α = 0.085 m^{-1} and ωc_o^{-1} = 8396.1 m^{-1}. Moreover, in the same experimental conditions: in ethanol, α = 0.197 m^{-1} and $\omega \cdot c_o^{-1}$ = 11004 m^{-1}; in 1,2-ethanediol, α = 0.615 m^{-1} and $\omega \cdot c_o^{-1}$ = 7594 m^{-1}; in carbon tetrachloride, α = 2.07 m^{-1} and $\omega \cdot c_o^{-1}$ = 13643 m^{-1}; and in 1,5-pentanediol, α = 4.11 m^{-1} and $\omega \cdot c_o^{-1}$ = 7904 m^{-1}. The data for the calculations were taken from the literature [2,5,22,23] or were measured during this study.

Therefore, taking into account the four RTILs experimentally investigated in this work, it should be clearly noted that in the given experimental conditions, the ultrasound absorption at low frequencies (i.e., at the frequencies used in typical speed of sound measurements, such as at 2 MHz) is also still small enough for the correct use of the Newton-Laplace relation. In other words, c_o may be still treated as a thermodynamic equilibrium property because the effect of absorption on the speed of sound is small and may be ignored (dissipative processes can be neglected). This results from the fulfilled inequality $\alpha \cdot c_o \cdot (2 \cdot \pi \cdot f)^{-1} << 1$, i.e., the left side values always lie in the range from $1.3 \cdot 10^{-4}$ (the lowest value - $[C_3mim][NTf_2]$ at 323.15 K) to $5.9 \cdot 10^{-4}$ (the highest value - $[C_6mim][NTf_2]$ at 293.15 K); generally speaking, over the whole investigated temperature range these values are in great part somewhat higher than for carbon

tetrachloride at 298.15 K ($1.52 \cdot 10^{-4}$) and lower than for 1,5-pentanediol at 298.15 K ($5.2 \cdot 10^{-4}$).

However, in many liquids, a relaxation process, or even several relaxation processes, are responsible for additional, often strong, increases of ultrasound absorption. In these highly attenuating conditions as well as in the border regions, particular care must be exercised because the relaxation processes cause not only absorption but also dispersion.[55,56] In the case of the four measured RTILs, the lowest f_{rel} values associated with ultrasound absorption are (169 and 172) MHz, which are observed for $[C_5mim][NTf_2]$ at 288.15 K and $[C_6mim][NTf_2]$ at 293.15 K, respectively; however, still lower f_{rel} values, are observed at room temperatures in the case of $[C_8mim][NTf_2]$ and $[C_4mim]_2[Co(NCS)_4]$) (Table S8). Since: (i) the relaxation frequency associated with the ultrasound absorption decreases with the decreasing temperature (and vice versa), (ii) the α/α_{cl} is small (in the range 1 to 3) and practically independent of temperature, and (iii) the temperature coefficient of ultrasound absorption is negative, the close similarity of ultrasound absorption in RTILs studied and associated molecular liquids is observed (the similarity was suggested already in our previous reports [1,2]). In other words, this is the same group according to liquid classification in relation to ultrasound absorption.[55] Since the relaxation frequency decreases with the increasing pressure in associated molecular liquids,[55,57] we can suppose with the great probability that both RTILs studied to date and generally all aprotic RTILs behave similarly. Obviously, it is only supposition, but it is plausible.

As mentioned in the introduction, knowledge of the relaxation regions is necessary to correctly use the acoustic method (based on the speed of sound measurements) to obtain related thermodynamic properties under high pressures because such studies must be done outside of the relaxation regions of the ultrasound velocity.[6-8] Unfortunately, this crucial condition can sometimes be overlooked. In other words, it should be keep in mind that for all aprotic RTILs studied to date, the determined f_{rel} decrease with the decreasing temperature

and increasing side alkyl chain length in 3-methylimidazolium cation,[1,2,3,and this work] and f_{rel} should decrease with the increasing pressure. Thus, care must be exercised when investigating RTILs in lower temperatures and/or higher pressures. For instance, for $[C_n mim][NTf_2]$ homologues, it is especially important beginning from $[C_6 mim][NTf_2]$, whereas in the case of $[C_n mim][PF_6]$ homologues, it begins even from $[C_4 mim][PF_6]$. In the case of $[C_n mim][PF_6]$, the clear dispersion symptoms are visible for $[C_6 mim][PF_6]$ and even more for $[C_8 mim][PF_6]$ already from temperatures near 300 K at atmospheric pressure because the measured speed of sound shows an increase of deviations from linearity (much more evident in the case of $[C_8 mim][PF_6]$) with the decreasing temperature.[3,58] In other words, the lower the temperature, the higher the increase of the speed of sound with the decreasing temperature (concave up curve) is observed, and it is typical behavior in dispersion regions.[54,55] In the case of $[C_8 mim][PF_6]$, an additional argument for existence of relaxation region in range of several MHz is connected with the shear relaxation spectra which indicate, for instance, the shear relaxation frequency already around 20 MHz at 298.15 K.[44] Therefore, in practice, it is always necessary to exercise caution whether the measured speed of sound in given experimental conditions (lower temperature and/or high pressure) can be indeed treated as the equilibrium thermodynamic quantity and used to determination of thermodynamic properties under high pressures by means of indirect acoustic route. It is especially important in the case of ILs showing high viscosities and/or rapid increase of viscosity with the decreasing temperature.

Because of the relatively large ultrasonic absorption in many RTILs, ultrasonic velocity is subject to a considerable dispersion. Fortunately, from the ultrasound absorption data, the frequency dependence of the ultrasonic velocity can be estimated.[55,59,60] Figures 8 and 9 show examples of the ultrasonic velocity dependence on frequency estimated from the absorption data by the use of the following relation:

$$\frac{c^2}{c_0^2} = 1 + \frac{c_0}{\pi} \cdot \sum_{i-1}^{n} \frac{A_i \cdot f_{rel,i}^{-1} \cdot f^2}{1 + (f^2 \cdot f_{rel,i}^{-2}) \cdot (1 - A_i \cdot c_0 \cdot f_{rel,i} \cdot \pi^{-1})} \qquad (12)$$

where A_i and $f_{rel,i}$ denotes the parameters obtained from the ultrasound absorption data. The n number is the same as in the case of the model used for description of the ultrasound absorption data, i.e., the use of Eq.3 (single Debye term) leads also to $n = 1$ in Eq.12. Thus, it is not surprising that frequency dependence of c is strongly correlated with the relaxation frequency (or frequencies) of the relevant absorption spectrum. From the eight RTILs for which the dispersion curves of ultrasonic velocities were estimated, $[C_4mim]_2[Co(NCS)_4]$ shows ultrasonic velocity dependence on frequency as early as above 7 MHz at 293.15 K. At the same temperature, $[C_6mim][NTf_2]$ shows such dependence above 28 MHz; however, with the increasing temperature, the dispersion region is shifted rapidly towards higher frequencies, i.e., above 100 MHz at 323.15 K. (Figure 9). At the same time the weakest dispersion (starting about 80 MHz at 293.15 K) shows $[C_2mim][NTf_2]$. As an indication of dispersion were taken into account the estimated values for which difference between these values and the determined experimentally speed of sound (c-c_o) exceeded expanded uncertainty of the experimental speed of sound equal ±1 $m \cdot s^{-1}$ ($U(c_o) = 0.5$ $m \cdot s^{-1}$, k = 2). Table 5 summarize the dispersion values c_∞/c_o obtained both indirectly from absorption measurements and directly from TG method. It is visible that the dispersion obtained indirectly are somewhat lower than those obtained from TG measurements. This discrepancy results probably from two basic reasons: (i) on the one hand, it is connected with the lack of the ultrasound absorption data above 300 MHz and fact that none of the absorption spectra reach the frequency independent high-frequency limit, what results in greater uncertainty of the estimated c values in the high frequency region, and especially c_∞; and (ii) on the other hand, the c values in the high frequency region along with limiting c_∞ values determined using TG method are also connected with relatively great uncertainty.

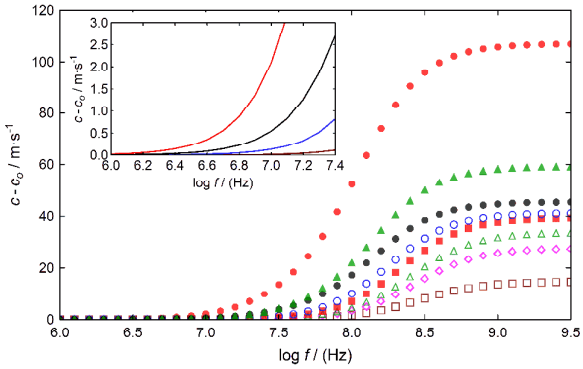

Figure 8. The ultrasound velocity dispersion at 293.15 K shown as difference $c - c_o$ plotted against log f for: □, $[C_2mim][NTf_2]$; ◊, $[C_3mim][NTf_2]$; Δ, $[C_4mim][NTf_2]$; ■, $[C_5mim][NTf_2]$; ○ $[C_6mim][NTf_2]$; ●, $[C_8mim][NTf_2]$; ▲, $[C_2mim]_2[Co(NCS)_4]$; and ●, $[C_4mim]_2[Co(NCS)_4]$. The inset shows dispersion beginning (in the increasing order) for: brown line, $[C_2mim][NTf_2]$; blue line, $[C_6mim][NTf_2]$; black line, $[C_8mim][NTf_2]$; and red line, $[C_4mim]_2[Co(NCS)_4]$.

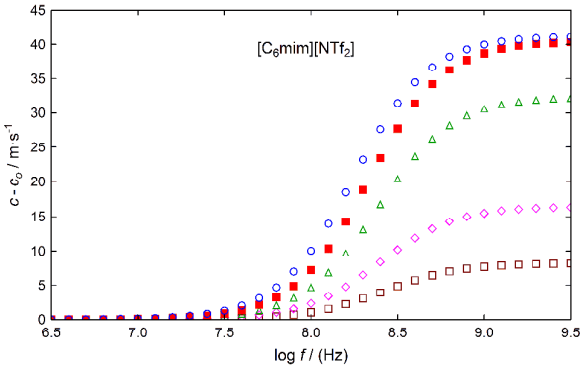

Figure 9. The ultrasound velocity dispersion shown as difference $c - c_o$ plotted against log f for $[C_6Mim][NTf_2]$ at temperatures; □, 323.15 K; ◊, 313.15 K; Δ, 303.15 K; ■, 298.15 K; and ○, 293.15 K.

Finally, we must explain that only originally calculated sets of parameters of ultrasound absorption spectra were discussed because of the small effect on these spectra resulting from consideration (or not) of the ultrasound dispersion.

Table 5

The Dispersion Values c_∞/c_o for Various RTILs at Temperature 298.15 K, Obtained Directly [a] from Measurements of the c_∞ and c_o Using TG Method as well as Indirectly [b] by Estimation from Ultrasound Absorption Measurements

RTIL	c_∞/c_o	Refs
$[C_4mim][BF_4]$	1.13 [a]	15
$[C_4mim][PF_6]$	1.16 [a]	15
	1.22 [a]	18
$[C_4m_2im][BF_4]$	1.14 [a]	15
$[C_2mim][NTf_2]$	1.008 [b]	This work
$[C_3mim][NTf_2]$	1.017 [b]	This work
$[C_4mim][NTf_2]$	1.024 [b]	This work
	1.07 [a]	15
	1.22	18
$[C_5mim][NTf_2]$	1.031 [b]	This work
$[C_6mim][NTf_2]$	1.033 [b]	This work
$[C_8mim][NTf_2]$	1.034 [b]	This work
$[C_2mim]_2\ [Co(NCS)_4]$	1.034 [b]	This work
$[C_4mim]_2\ [Co(NCS)_4]$	1.059 [b]	This work
$[N_{1,1,1,3}][NTf_2]$	1.26 [a]	18

5. CONCLUSIONS

Frequency-dependent absorption is the characteristic acoustic property because the

experimental data clearly do not show a constant α/f^{-2} but instead exhibit that $d(\alpha/f^{-2})/df < 0$. In the investigated temperature range, $d(\alpha/f^{2})/dT < 0$ is observed as well. Moreover, the results show that lengthening the side alkyl chain in 1-alkyl-3-methylimidazolium cations does not show a significant effect on the speed of sound but significantly affects the ultrasound absorption spectra (both relaxation amplitude and relaxation frequency). Whereas the relaxation frequency decreases with the increasing chain length, i.e., with the increasing of the nonpolar part of the cation, the magnitude of α/f^{-2} clearly increases regularly with the increasing length of the side alkyl chain of the 1-alkyl-3-methylimidazolium ring. From the $[C_n mim][NTf_2]$ measured in this work and the literature data, the highest absorption and lowest relaxation frequency were observed for $[C_8 mim][NTf_2]$. All of the findings can be generally attributed to the clear shift in balance between the polar part and the non-polar part of the imidazolium cations. Lengthening the side alkyl chain of the imidazolium cation increases the non-polar part of the cation and consequently leads to the increase of the entire nonpolar domain. It should also be noted that the longer the carbon chain, the more important the internal motion of the molecule with respect to the Coulomb interactions as well as to the possible hydrogen bonding association. Qualitatively, the described behavior is independent of the anion because the literature data on ultrasound absorption for $[C_n mim][PF_6]$ and $[C_n mim]_2[Co(NCS)_4]$ analyzed in this work suggested the same results; however, for the same cation, the magnitude of α/f^{-2} in the non-relaxation region below the relaxation frequency is clearly lower in the case of the $[NTf_2]^-$ anion in comparison with the $[PF_6]^-$ anion. In other words, $[C_n mim][NTf_2]$ showed a lower absorption than adequate $[C_n mim][PF_6]$. Thus, the energy dissipation associated with both the classical and non-classical contributions increases with the increasing alkyl chain length of the 1-alkyl-3-methylimidazolium cation and with change of the anion from $[NTf_2]^-$ to the $[PF_6]^-$. Furthermore, these RTILs show mostly both the structural and shear relaxation processes. Thus, the results of the ultrasound absorption

investigations (longitudinal wave) are consistent with the literature reports on shear relaxation spectra (transversal (shear) wave).

The analysis of the ultrasound velocity dispersion for $[C_nmim][NTf_2]$ and $[C_nmim]_2[Co(NCS)_4]$ shows that in experimental conditions dispersion is already present at relatively low megahertz frequencies; the strongest shows $[C_4mim]_2[Co(NCS)_4]$ starting already from frequency above 7 MHz at 293.15 K, whereas the weakest shows $[C_2mim][NTf_2]$ starting from frequency in the vicinity of 80 MHz.

An additional analysis of the effect of ultrasound absorption on the speed of sound showed that in the given experimental conditions, the use of the Newton-Laplace relation to determine the thermodynamic properties is rather well-founded and correct. However, at lower temperatures and/or higher pressures special care must be exercised. Generally, special care must be exercised when the speed of sound measurements are planned/or made for RTILs showing high, or extremely high viscosities. In such situations, the measurements in a broader temperature range, especially also at higher temperatures, are suggested, and next the linearity should be checked and analyzed. It is the simplest and also a plausible solution in the case of the controversy on the presence of strong dissipative processes during the ultrasound wave propagation.

ASSOCIATED CONTENT

Supporting Information

Characterization, structure and synthesis of $[C_nmim][NTf_2]$ (n = 3,4,5,6), the raw values of speed of sound, density, viscosity (kinematic and static shear), quotient αf^{-2}, activation energy E_α, isentropic compressibility coefficient and molar isentropic compressibility as well as refitting results reported in refs 1 and 2 data for $[C_8mim][NTf_2]$ and $[C_nmim]_2[Co(NCS)_4]$ (n = 2,4) by the use of model with two Debye terms. This material is available free of charge via the internet at http://pubs.acs.org.

Notes

The authors declare no competing financial interest.

Acknowledgments

The authors are grateful to Mr. A. Praski for the viscosity measurement.

REFERENCES

1. Hensel-Bielówka, S.; Wojnarowska, Ż.; Dzida, M.; Zorębski, E.; Zorębski, M.; Geppert-Rybczyńska, M.; Peppel, T.; Grzybowska, K.; Wang, Y.; Sokolov, A. P.; Paluch, M. Heterogeneous Nature of Relaxation Dynamic of Room Temperature Ionic Liquids $(EMim)_2[Co(NCS)_4]$ and $(BMim)_2[Co(NCS)_4]$. *J. Phys. Chem. C* **2015**, *119*, 20363-20368.
2. Zorębski, E.; Geppert-Rybczyńska, M.; Zorębski, M. Acoustics as a Tool for Better Characterization of Ionic Liquids: A Comparative Study of 1-Alkyl-3-Methyl-Imidazolium Bis[(trifluoromethyl)sulfonyl]imide Room-Temperature Ionic Liquids. *J. Phys. Chem. B* **2013***, 117*, 3867-3876.
3. Makino, W.; Kishikawa, R.; Mizoshiri, M.; Takeda, S.; Yao, M. Viscoelastic Properties of Room Temperature Ionic Liquids. *J. Chem. Phys.* **2008**, *129*, 104510.
4. Mirzaev, S. Z.; Kaatze, U. Critical Concentration Fluctuations in the Ionic Binary Mixture Ethylammonium Nitrate – n-Octanol: An Ultrasonic Spectrometry Study. *Phys. Rev. E* **2002***, 65,* 021509.
5. Kaatze, U.; Hushcha, T.O.; Eggers, F. Ultrasonic Broadband Spectrometry of Liquids: A Research Tool in Pure and Applied Chemistry and Chemical Physics. *J. Solution Chem*. **2000**, *29*, 299-367.
6. Matheson, A. J. *Molecular Acoustics*; Wiley, New York, 1971.
7. Wilhelm, E. What You Always Wanted to Know about Heat Capacities, but Were Afraid to Ask. *J. Solution Chem*. **2010**, *39***,** 1777-1818.
8. Zorębski, E.; Dzida, M. The Effect of Temperature and Pressure on Acoustic and Thermodynamic Properties of 1,4-Butanediol. The Comparison with 1,2- and 1,3-Butanediols. *J. Chem. Thermodyn.* **2012**, *54*, 100-107.

9. Cobb, W. N. Finite-Amplitude Method for the Determination of the Acoustic Nonlinearity Parameter *B*/*A*. *J. Acoust. Soc. Am*. **1983**, *73*, 1525-1531.

10. Frez, C.; Diebold, G. J.; Tran, C. D.; Yu, S. Determination of Thermal Diffusivities, Thermal Conductivities, and Sound Speeds of Room-Temperature Ionic Liquids by the Transient Grating Technique. *J. Chem. Eng. Data* **2006**, *51*, 1250-1255.

11. Kozlov, D. M.; Kiefer, J.; Seeger, T.; Fröba, A. P; Leipertz, A. Simultaneous Measurement of Speed of Sound, Thermal Diffusivity, and Bulk Viscosity of 1-Ethyl-3-Methylimidazolium-Based Ionic Liquids Using Laser-Induced Gratings. *J. Phys. Chem. B* **2014***, 118*, 14493-14501.

12. Marsh, K. N.; Boxall, J. A.; Lichtenthaler, R. Room Temperature Ionic Liquids and Their Mixtures - a Review. *Fluid Phase Equilib*. **2004**, *219*, 93–98.

13. Hayes, R.; Warr, G. G.; Atkin, R. Structure and Nanostructure in Ionic Liquids. *Chem. Rev.* **2015**, *115*, 6357-6426.

14. Eichler, H. J.; Gunter, P.; Pohl, D. W. *Laser-Induced Dynamic Gratings*; Springer-Verlag, Berlin, 1986.

15. Fukuda, M.; Kajimoto, O.; Terazima, M.; Kimura, Y. Application of the Transient Grating Method to the Investigation of the Photo-Thermalization Process of Malachite Green in Room Temperature Ionic Liquids. *J. Mol. Liquids* **2007**, *134*, 49-54.

16. Demizu, M.; Terazima, M.; Kimura, Y. Transport Properties of Binary Mixtures of Carbon Dioxide and 1-Butyl-3-Methylimidazolium Hexafluorophosphate Studied by Transient Grating Spectroscopy. *Anal.Sci.* **2008**, *24*,1329-1334.

17. Demizu, M.; Harada, M.; Saijo, K.; Terazima, M.; Kimura, Y. Transport properties and solvation structure of mixtures of carbon dioxide and room-temperature ionic liquids *Bull. Chem. Soc. Jpn.* **2011**, *84*, 70–78.

18. Fukuda, M; Terazima, M.; Kimura, Y. Sound Velocity Dispersion in Room Temperature Ionic Liquids Studied Using the Transient Grating Method. *J. Chem. Phys*. **2008**, *128*, 114508.

19. Kozlov, D. N.; Kiefer, J.; Seeger, T.; Fröba, A. P.; Leipertz, A. Determination of Physicochemical Parameters of Ionic Liquids and Their Mixtures with Solvents Using Laser-Induced Gratings. *J. Phys. Chem. B* **2011***, 115,* 8528–8533.

20. Chirico, R. D.; Diky, V.; Magee, J. W.; Frenkel, M.; Marsh, K. N. Thermodynamic and Thermophysical Properties of the Reference Ionic Liquid: 1-Hexyl-3-Methylimidazolium Bis[(trifluoromethyl)sulfonyl]amide (Including Mixtures). Part 2.Critical Evaluation and Recommended Property Values (IUPAC Technical Report). *Pure and Applied Chemistry* **2009**, *81*, 791-828.

21. Skowronek, J.; Geppert-Rybczyńska, M.; Jacquemin, J.; Goodrich, P.; Vicente, J. A.; Chorążewski, M.; Jężak, S.; Zorębski, M.; Zorębski, E.; Żarska, M.; et al. Acoustic and Volumetric Properties of Diluted Solutions of Water in Ionic Liquids. *J. Solution Chem*. **2015**, *44*, 824-837.

22. Zorębski, E.; Zorębski, M.; Geppert-Rybczyńska, M. Ultrasonic Absorption Measurements by Means of a Megahertz-Range Measuring Set. *J. Phys. IV* **2006**, *137*, 231-236.

23. Zorębski, E.; Zorębski, M. A Comparative Ultrasonic Relaxation Study of Lower Vicinal and Terminal Alkanediols at 298.15 K in Relation to Their Molecular Structure and Hydrogen Bonding. *J. Phys. Chem. B* **2014**, *118*, 5934-5942.

24. Dzida, M.; Chorążewski, M.; Zorębski, M.; Mańka, R. Modifications of a High Pressure Device for Speed of Sound Measurements in Liquids. *J. Phys. IV* **2006**, *137*, 203-207.

25. Zorębski, E.; Zorębski, M.; Ernst, S. Speed of Ultrasound in Liquids Measured at Constant Acoustic Pathlegth. Comparison and Disscusion of Errors. *J. Phys. IV* **2005**, *129*, 79-82.

26. Nascimento, M. L. F.; Aparicio, C. Data Classification with the Vogel-Fulcher-Tamman-Hesse Viscosity Equation Using Correspondence Analysis. *Physica B* **2007**, *398*, 71-77.

27. Böhmer, R.; Ngai, K. L.; Angell, C. A. Nonexponential Relaxations in Strong and Fragile Glass Formers. *J. Chem. Phys*. **1999**, *99*, 4201-4209.

28. Angell, C.A. in: *Relaxation in Complex Systems*, ed. by Ngai, K.L, Wright, G.B. NRL, Washington, D.C., 1985.

29. Wu, K-J.; Chen, Q-L.; He, C-H. Speed of Sound of Ionic Liquids: Database, Estimation, and Its Application for Thermal Conductivity Prediction. *AIChE. J*. **2014**, *60*, 1120-1131.

30. Gómez, E.; Calvar, N.; Macedo, E. A.; Domínguez, Á. Effect of the Temperature on the Physical Properties of Pure 1-Propyl-3-Methylimidazolium Bis[(trifluoromethyl)sulfonyl]-Imide and Characterization of Its Binary Mixtures with Alcohols. *J. Chem. Thermodyn*. **2012**, *45*, 9-15.

31. Gomes de Azevedo, R. G.; Esperança, J. M. S. S.; Szydlowski, J.; Visak, Z. P.; Pires, P. F.; Guedes, H. J. R.; Rebelo, L. P. N. Thermophysical And Thermodynamic Properties of Ionic Liquids Over an Extended Pressure Range: [Bmim][NTf_2] And [Hmim][NTf_2]. *J. Chem. Thermodyn.* **2005**, *37*, 888-899.

32. Geppert-Rybczyńska, M.; Sitarek, M. Acoustic and Volumetric Properties of Binary Mixtures of Ionic Liquid 1-Butyl-3-Methylimidazolium Bis[(trifluoromethyl)sulfonyl] imide with Acetonitrile and Tetrahydrofuran *J. Chem. Eng. Data* **2014**, *59*, 1213-1224.

33. Seoane, R. G.; Corderí, S.; Gómez, E.; Calvar, N.; González, E. J.; Macedo, E. A.; Domínguez, Á. Temperature Dependence and Structural Influence on the Thermophysical

Properties of Eleven Commercial Ionic Liquids. *Ind. Eng. Chem. Res.* **2012**, *51*, 2492-2504.

34. Gonzáles, E. J.; Domínguez, Á.; Macedo, E. A. Excess Properties of Binary Mixtures Containing 1-Hexyl-3-Methylimidazolium Bis[(trifluoromethyl)sulfonyl]imide Ionic Liquid and Polar Organic Compounds. *J. Chem. Thermodyn*. **2012**, *47*, 300-311.
35. Widegren, J. A.; Magee, J. W. Density, Viscosity, Speed of Sound, and Electrolytic Conductivity for the Ionic Liquid 1-Hexyl-3-Methylimidazolium Bis[(trifluoromethyl)sulfonyl]imide and Its Mixtures with Water. *J. Chem. Eng. Data* **2007**, 52, 2331-2338.
36. Johansson, P.; Gejji, S. P.; Tegensfeldt, J.; Lindgren, J. The Imide Ion: Potential Energy Surface and Geometries. *Electrochim.Act*a **1998**, *43*, 1375-1379.
37. Fuji, K.; Fujimori, T.; Takamuku, T.; Kanzaki, R.; Umebayashi, Y.; Ishigaro, S. Conformational Equilibrium of Bis[(trifluoromethane)sulfonyl]imide Anion of a Room-Temperature Ionic Liquid: Raman Spectroscopic Study and DFT Calculations. *J. Phys. Chem. B* **2006**, *110*, 8179-8183.
38. Fumino, K.; Reimann, S.; Ludwig, R. Probing Molecular Interaction in Ionic Liquids by Low Frequency Spectroscopy: Coulomb Energy, Hydrogen Bonding and Dispersion Forces. *PCCP* **2014**, *16*, 21903-21929.
39. Fumino, K.; Wulf, A.; Ludwig, R. The Potential Role of Hydrogen Bonding in Aprotic and Protic Ionic Liquids. *PCCP* **2009**, *11*, 8790-8794.
40. Yamamoto, K.; Tani, M.; Hangyo, M. Terahertz time-domain spectroscopy of imidazolium ionic liquids. *J. Phys. Chem. B* **2007**, *111*, 4854-4859.
41. Schröder, U.; Wadhawan, J. D.; Compton, R. G.; Marken, F.; Suarez, P. A. Z.; Consorti, C. S.; de Souza, R. F.; Dupont, J. Water-Induced Accelerated Ion Diffusion: Voltammetric Studies in 1-Methyl-3-[2,6-(S)-Dimethylocten-2-yl]Imidazolium Tetrafluoroborate, 1-

Butyl-3-Methylimidazolium Tetrafluoroborate and Hexafluorophosphate Ionic Liquids. *New. J. Chem.* **2000**, *24*, 1009-1015.

42. Canongia Lopes, J. N. A.; Padua, A. A. H. Nanostructural Organization in Ionic Liquids, *J. Phys. Chem. B* **2006**, *110*, 3330-3335.
43. Kofu. M.; Nagao, M.; Ueki, T.; Kitazawa, Y.; Nakamura, Y.; Sawamura, S.; Watanabe, M.; Yamamuro, O. Heterogeneous Slow Dynamics of Imidazolium-Based Ionic Liquids Studied by Neutron Spin Echo. *J. Phys. Chem. B* **2013**, *117*, 2773-2781.
44. Yamaguchi, T.; Mikawa, K.; Koda, S.; Fujii, K.; Endo, H.; Shibayama, M.; Hamano, H.; Umebayashi, Y. Relationship Between Mesoscale Dynamics and Shear Relaxation of Ionic Liquids with Long Alkyl Chain. *J. Chem. Phys*. **2012**, *137*, 10451.
45. Ge, R.; Hardacre, C.; Jacquemin, J.; Nancarrow, P.; Rooney D. W. Heat Capacities of Ionic Liquids as a Function of Temperature at 0.1 MPa. Measurement and Prediction. *J. Chem. Eng. Data* **2008**, *53*, 2148-2153.
46. Rassing, J.; Lassen, H. Analysis and Kinetic Interpretation of Ultrasonic Absorption Spectra. *Acta Chem. Scand*. **1969**, *23*, 1007-1016.
47. Kobryn, A. E.; Hirata, F. Statistical-Mechanical Theory of Ultrasonic Absorption in Molecular Liquids. *J. Chem. Phys*. **2007**, *126*, 044504.
48. Weingärtner, H.; Sasisanker, P.; Daguenet, C.; Dyson, P. J.; Krossing, I.; Slattery, J. M.; Schubert, T. The Dielectric Response of Room-Temperature Ionic Liquids: Effect of Cation Variation. *J. Phys. Chem. B* **2007**, *111*, 4775-4780.
49. Wuensch, B. J.; Hueter, T. F.; Cohen, M. S. Ultrasonic Absorption in Castor Oil: Deviations from Classical Behavior. *J. Acoust. Soc. Am*. **1956**, *28*, 311-312.
50. Behrens, R.; Kaatze, U. Hydrogen Bonding and Chain Conformational Isomerization of Alcohols Probed by Ultrasonic Absorption and Shear Impedance Spectrometry. *J. Phys. Chem*. *A* **2001**, *105*, 5829-5835.

51. Yamaguchi, T.; Nakahara, E.; Koda, S. Quantitative Analysis of Conductivity and Viscosity of Ionic Liquids in Terms of Their Relaxation Times. *J. Phys. Chem. B* **2014**, *118*, 5752-5759.

52. Yamaguchi, T.; Miyake, S.; Koda, S. Shear Relaxation of Imidazolium-Based Room-Temperature Ionic Liquids. *J. Phys. Chem. B* **2010**, *114*, 8126-8133.

53. Dukhin, A. S.; Goetz, P. J. Bulk Viscosity and Compressibility Measurement Using Acoustic Spectroscopy. *J. Chem. Phys*. **2009**, *130*, 124519.

54. Litovitz, T. A.; Davis, C. M. *Structural and Shear Relaxation in Liquids.* In Physical Acoustic.; Mason, W.P., Ed.; Academic Press, New York, 1965, Vol. II, Part A.

55. Herzfeld, K. F.; Litovitz, T. A. *Absorption and dispersion of ultrasonic waves*; Academic Press, New York, 1959.

56. Bhatia, A.B. *Ultrasonic absorption*; Oxford University Press, London, 1967.

57. Litovitz, T. A.; Carnevale, E. H.; Kendall, P. A. Effects of Pressure on Ultrasonic Relaxation in Liquids. *J. Chem. Phys*. **1957**, *26*, 465-468.

58. Pereiro, A. B.; Legido, J. L.; Rodrigues, A. Physical Properties of Ionic Liquids Based on 1-Alkyl-3-Methylimidazolium Cation and Hexafluorophosphate as Anion and Temperature Dependence. *J. Chem. Thermodyn*. **2007**, *39*, 1168-1175.

59. Bauer, G. *Properties of Gases, Liquids, and Solutions*. In Physical Acoustic.; Mason, W.P. Ed.; Academic Press, New York, 1965, Vol. II, Part A.

60. Wald, E.; Kaatze, U. Chain Dynamics of Ethylene Oxide Oligomer Melts. An Ultrasonic Spectroscopy Study. *J. Phys. Chem. B* **2014**, *118*, 13300-13311.

TOC

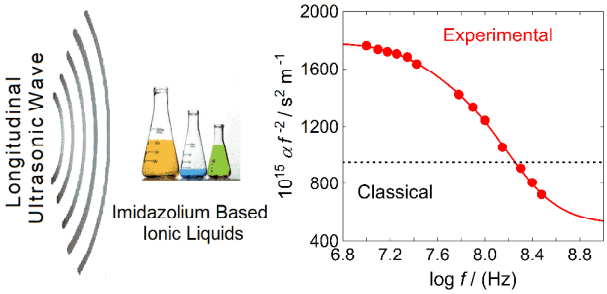
Longitudinal
Ultrasonic Wave
Imidazolium Based
Ionic Liquids
Experimental
Classical
2000
1600
1200
800
400
6.8
7.2
7.6
8.0
8.4
8.8
log f / (Hz)
10^15 α f^-2 / s^2 m^-1

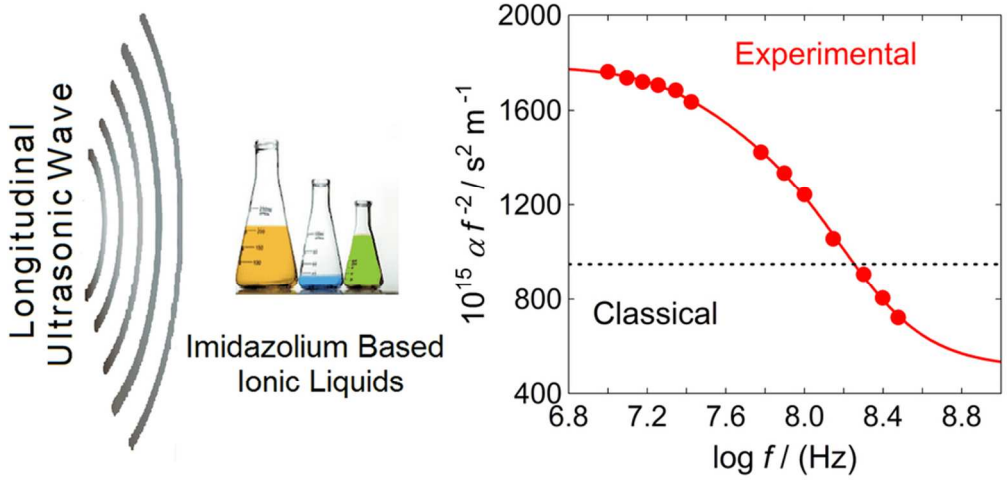

TOC
41x20mm (600 x 600 DPI)